Report

Current Biology

Aurora A Kinase Contributes to a Pole-Based Error Correction Pathway

Graphical Abstract

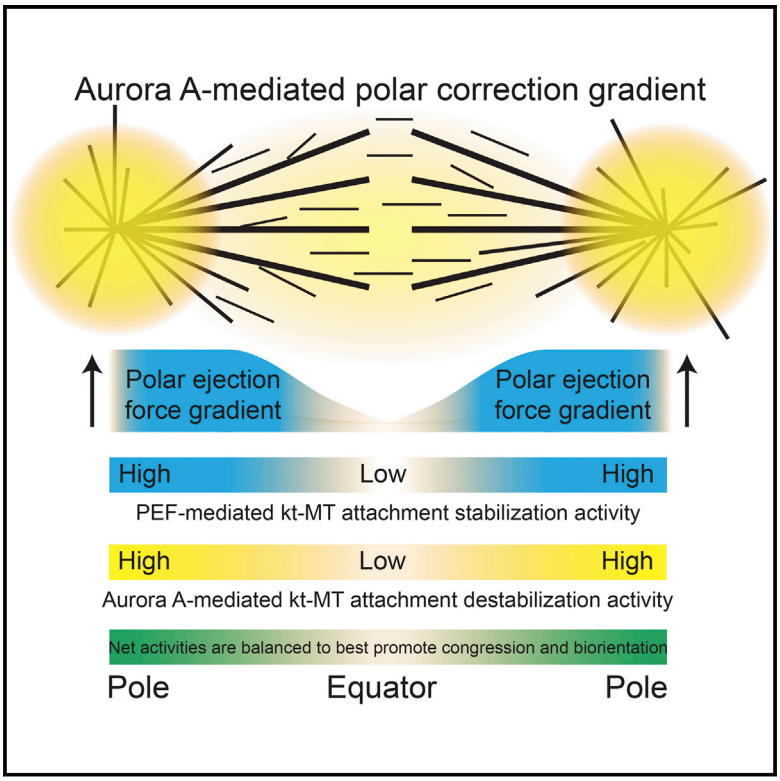

Authors

Anna A. Ye, Jovana Deretic, Christopher M. Hoel, Albert W. Hinman, Daniela Cimini, Julie P. Welburn, Thomas J. Maresca

Correspondence

tmaresca@bio.umass.edu

In Brief

Error correction, which requires the destabilization of improper kinetochore-microtubule attachments, often takes place near spindle poles, but the significance of this location was unclear. Ye et al. show that Aurora A kinase facilitates error correction through a pole-centered activity gradient that locally phosphorylates kinetochore substrates.

Highlights

- An AAK activity gradient in *Drosophila* S2 cells counters the effects of elevated PEFs
- AAK phosphorylates kinetochores and destabilizes attachments near poles in S2 cells
- AAK is required for efficient error correction in *Drosophila* and mammalian cells
- AAK phosphorylates the core kinetochore-MT attachment factor Ndc80/Hec1 in human cells

Ye et al., 2015, Current Biology *25*, 1842–1851
July 20, 2015
http://dx.doi.org/10.1016/j.cub.2015.06.021

CellPress

Current Biology
Report

Aurora A Kinase Contributes to a Pole-Based Error Correction Pathway

Anna A. Ye,[1,2] Jovana Deretic,[3] Christopher M. Hoel,[1] Albert W. Hinman,[4] Daniela Cimini,[4] Julie P. Welburn,[3] and Thomas J. Maresca[1,2,*]

[1]Biology Department, University of Massachusetts Amherst, Amherst, MA 01003, USA
[2]Molecular and Cellular Biology Graduate Program, University of Massachusetts Amherst, Amherst, MA 01003, USA
[3]Wellcome Trust Centre for Cell Biology, School of Biological Sciences, University of Edinburgh, Edinburgh EH9 3JR, UK
[4]Department of Biological Sciences and Virginia Bioinformatics Institute, Virginia Tech, Blacksburg, VA 24061, USA
*Correspondence: tmaresca@bio.umass.edu
http://dx.doi.org/10.1016/j.cub.2015.06.021

SUMMARY

Chromosome biorientation, where sister kinetochores attach to microtubules (MTs) from opposing spindle poles, is the configuration that best ensures equal partitioning of the genome during cell division. Erroneous kinetochore-MT attachments are commonplace but are often corrected prior to anaphase [1, 2]. Error correction, thought to be mediated primarily by the centromere-enriched Aurora B kinase (ABK) [3–5], typically occurs near spindle poles [6]; however, the relevance of this locale is unclear. Furthermore, polar ejection forces (PEFs), highest near poles [7], can stabilize improper attachments by pushing mal-oriented chromosome arms away from spindle poles [8, 9]. Hence, there is a conundrum: erroneous kinetochore-MT attachments are weakened where PEFs are most likely to strengthen them. Here, we report that Aurora A kinase (AAK) opposes the stabilizing effect of PEFs. AAK activity contributes to phosphorylation of kinetochore substrates near poles and its inhibition results in chromosome misalignment and an increased incidence of erroneous kinetochore-MT attachments. Furthermore, AAK directly phosphorylates a site in the N-terminal tail of Ndc80/Hec1 that has been implicated in reducing the affinity of the Ndc80 complex for MTs when phosphorylated [10–12]. We propose that an AAK activity gradient contributes to correcting mal-oriented kinetochore-MT attachments in the vicinity of spindle poles.

RESULTS

Bioriented attachments are thought to be stabilized, in part, by tension-dependent movements [13, 14] of outer kinetochore components away from ABK. The resultant spatial separation correlates with a reduction in phosphorylation of kinetochore-microtubule (MT) attachment factors [15, 16] that is proposed to increase the kinetochore's affinity for MTs [17]. Flawed attachments are weakened in favor of bioriented kinetochores through a process called error correction. Many models evoke tension-dependent inhibition of centromere (CEN)-based error correction via spatial separation [18]. The concept is reasonable if erroneous attachments are "tensionless," yet improper attachments may come under tension when mal-oriented chromosomes are opposed by polar ejection forces (PEFs) [19]. In support of this, we previously reported that elevated PEFs stabilize syntelic attachments [8], where sister kinetochores attach to the same pole, by overwhelming Aurora B kinase (ABK). Thus, while CEN-based models explain the instability of tensionless attachments, they fail to account for error correction when PEF-generated tension opposes ABK. Furthermore, recent work suggests that CEN-based Aurora kinase is dispensable for error correction in budding yeast, as mutants with Ipl1 (*S.c.* Aurora homolog) enriched on the spindle rather than the centromeres still achieved biorientation [20]. Clearly, a more comprehensive understanding of error correction requires further inquiry.

Unlike budding yeast, metazoans possess multiple Aurora kinases, most notably ABK and Aurora A kinase (AAK), which are enriched at centromeres and spindle poles/centrosomes, respectively [21]. As the kinases share nearly identical consensus target motifs [22], it is likely that the principal determinant of their substrate specificity is their respective sub-cellular localizations [23]. Here, we investigate whether a non-CEN-based pathway contributes to error correction by testing the hypothesis that AAK phosphorylates kinetochore substrates in the vicinity of poles.

We previously developed a cell-based assay in which tension can be experimentally elevated at kinetochores by manipulating PEF production [8]. In the PEF assay, inducible overexpression of the major PEF-producing kinesin-10 motor NOD [24] results in a dose-dependent increase in stable syntelic attachments in *Drosophila* S2 cells. To examine whether AAK affects the ability of PEFs to stabilize syntelic attachments, we created a cell line in which both NOD and AAK could be overexpressed simultaneously via $CuSO_4$ induction (Figure 1A and Movie S1). AAK-GFP localized to spindle MTs to varying degrees depending on the level of overexpression and was always highly enriched at centrosomes (Figures 1B and 1C). In agreement with previous observations in HeLa cells [25], the centrosome-enriched population of AAK-GFP turned over with rapid kinetics ($t_{1/2}$ of 7 s) in S2 cells (Figures S1A and S1B and Movie S2). Inducible NOD-mCherry and AAK-GFP cells co-expressing Ndc80-GFP, for assessment of attachment states, were subjected to the PEF

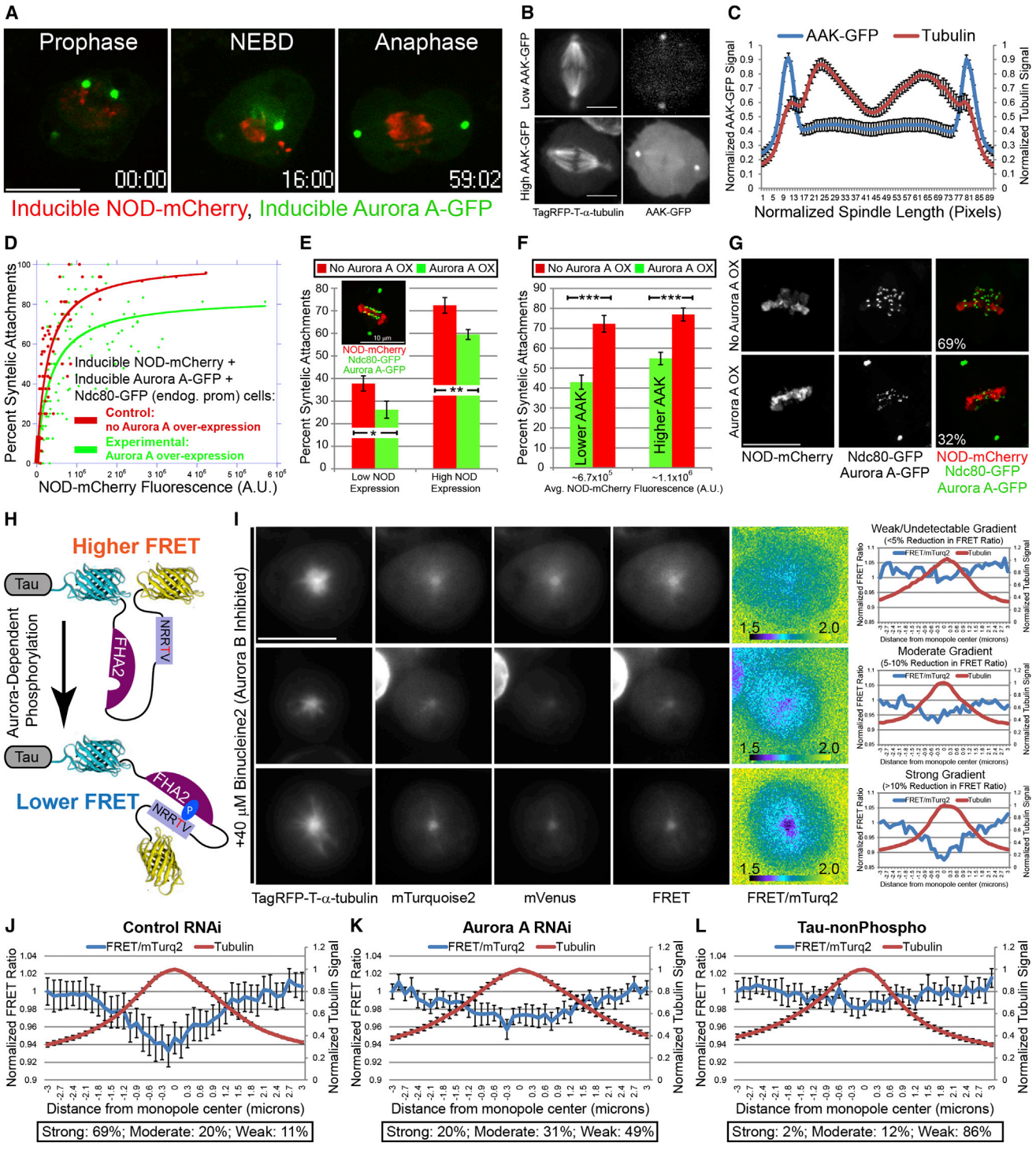

Figure 1. AAK Activity Is Highest near Spindle Poles and Counteracts the Kinetochore-MT Attachment Stabilizing Effect of Elevated PEFs

(A) Still frames from a time-lapse of a dividing S2 cell expressing inducible NOD-mCherry and inducible AAK-GFP.

(B) Spinning-disk confocal images showing examples of low (top) and high (bottom) AAK-overexpressing cells. MT localization is more evident in the higher expressing cell.

(C) Normalized fluorescence intensities of AAK-GFP and TagRFP-T-α-tubulin along the length of 14 mitotic spindles (normalized for variability in spindle length) from cells with a range of AAK-GFP overexpression. AAK-GFP is most abundant at centrosomes and its levels are slightly higher closer to the spindle poles than in the mid-spindle.

(legend continued on next page)

assay. Cells with and without AAK-GFP expression on the same coverslip could be compared due to variability in expression levels. Importantly, AAK overexpression reduced the potency of the PEF effect (Figures 1D–1G). Thus, AAK overexpression attenuates the kinetochore-MT attachment stabilizing effects of elevated PEFs in S2 cells.

The observation that centrosomal/spindle-pole-enriched AAK affected kinetochore-MT attachment stability suggested that the kinase could phosphorylate substrates at a distance through an activity gradient. A fluorescence resonance energy transfer (FRET)-based sensor that exhibits changes in intramolecular FRET upon phosphorylation [26] was used to probe this possibility. In the reporter used here, Aurora kinase phosphorylation causes a structural rearrangement such that phosphorylation leads to reduced FRET efficiency [27], and a prior strategy [28] was adapted to target the reporter to MTs in S2 cells (Figure 1H). To isolate the contribution of AAK to probe phosphorylation, we treated cells co-expressing TagRFP-T-α-tubulin and the Tau-Aurora FRET reporter with a high dose (40 μM) of the *Drosophila* ABK-specific inhibitor binucleine 2 [29, 30]. This treatment, which requires the addition of MG132 to prevent mitotic exit, results in monopolar spindle assembly in a majority of cells. Three categories of FRET emission ratios at the monopole center, as defined by TagRFP-T-α-tubulin signal, relative to ~3 μm away emerged when FRET of the MT-associated reporter was examined across monopoles (Figure 1I): weak/undetectable gradients (<5% reduction in FRET ratio), moderate gradients (5%–10% reduction), and strong gradients (>10% reduction). AAK activity was required for FRET-based visualization of the gradients, as depletion of AAK (Figures S1C–S1E) led to a reduction in the number of cells with strong gradients relative to control RNAi-treated cells (Figures 1J and 1K) and most AAK-depleted cells had weak/undetectable gradients (Figure 1K). A substantial majority of cells (86%) did not have detectable gradients in cells expressing a non-phosphorylatable (negative control) version of the reporter (Figure 1L). Thus, a pole-centered AAK phosphorylation gradient is present in mitotic *Drosophila* S2 cells.

While PEFs act on chromosome arms, it is the transmission of opposing force through the mis-attached kinetochores that leads to their stabilization. Thus, we reasoned that the AAK activity gradient counteracts the PEF effect by targeting kinetochore substrates that approach the spindle poles. To test this hypothesis, we adapted a strategy previously used to target the Aurora kinase FRET sensor to human kinetochores [15] for use in *Drosophila* S2 cells by fusing the FRET reporter to the C terminus of TagRFP-T-tagged *Drosophila* Mis12, a component of the core kinetochore-MT attachment complex [10] (Figure 2A). We confirmed earlier findings from HeLa cells [15] that the sensor is more phosphorylated (lower emission ratio) at unattached kinetochores than at bioriented kinetochores in *Drosophila* S2 cells (Figures 2B and 2C). Cells treated with binucleine 2 (Figure S1F) exhibited reduced sensor phosphorylation at unattached kinetochores (Figures 2B and 2C). The FRET measurements in binucleine 2-treated cells most likely underestimate the reduction in phosphorylation, given that a non-phosphorylatable reporter, which has equally high emission ratios at bioriented and unattached kinetochores, exhibited a 5% reduction in FRET in the presence of 40 μM binucleine 2 (Figures S2A and S2B). Taken together, the data suggest that ABK is the dominant kinase targeting the Mis12-FRET sensor at unattached kinetochores in S2 cells.

Sensor phosphorylation at aligned and polar kinetochores was evaluated next. The *Drosophila* CENP-E homolog (CENP-meta) was depleted from cells expressing the kinetochore-targeted FRET sensor to increase the number of polar chromosomes [31]. The FRET sensor was more phosphorylated at polar kinetochores than at bioriented kinetochores (Figures 2D, 2E, and S2C). Since polar chromosomes in CENP-E-depleted mouse fibroblasts have been shown to lack kinetochore-MT attachments [32], the increased phosphorylation observed at these kinetochores may have solely been a result of ABK-mediated phosphorylation of unattached kinetochores. However, this was not the case, as double depletion of CENP-meta and AAK, which did not reduce ABK activity (Figures S2D and S2E), resulted in a reduction in phosphorylation of the reporter at polar kinetochores relative to those in CENP-meta RNAi cells (Figures 2D, 2E, and Figure S2C). The data do not rule out a role for ABK in phosphorylating polar kinetochores in S2 cells, which may account for the statistically significant increase in phosphorylation of the reporter at polar versus aligned kinetochores that

(D) Plots of percent syntelic attachments versus NOD-mCherry fluorescence for cells with (green) and without (red) AAK-GFP overexpression. PEF-mediated stabilization of syntelic attachments is less potent in AAK-GFP-overexpressing cells. Data from six independent experiments were fit with a hyperbolic function. Control, n = 64 cells; AAK overexpression, n = 117 cells. R values are 0.81 (no AAK overexpression) and 0.72 (AAK overexpression).

(E) Mean percent syntelic attachments for low and high NOD-expressing cells, defined by the halfway point of the expression range in control cells, in control versus AAK-GFP-overexpressing (inset) cells. The percentage of syntelic attachments is significantly lower in AAK-overexpressing cells than in control cells at low and high NOD expression levels.

(F) AAK-GFP levels were quantified and the mean percent of syntelic attachments in cells from both the lower and upper half of the AAK-GFP overexpression range are significantly lower than groupings of control cells with comparable levels of NOD overexpression.

(G) Maximum-intensity projections of Ndc80-GFP (green)- and NOD-mCherry (red)-expressing cells with and without overexpressed AAK-GFP (green) but with comparable levels of NOD-mCherry. The percentage of syntelic attachments, which is lower in the AAK-GFP-overexpressing cell, is shown in the merged images.

(H) Schematic of the MT-targeted Tau-Aurora FRET sensor used in this study.

(I) Representative images of cells co-expressing TagRFP-T-α-tubulin and the Tau-Aurora FRET reporter treated with binucleine 2 and MG132. The FRET emission ratio images "FRET/mTurq2" are pseudo-colored, and the color wedge spans ratio values of 1.5 (black) to 2.0 (yellow). Examples of cells with "weak/undetectable" (<5% reduction), "moderate" (5%–10% reduction), and "strong" (>10% reduction) gradients as defined by the percent reduction in normalized FRET emission ratio in the monopole center relative to 3 μm away are shown.

(J–L) Normalized FRET ratios across monopoles (normalized tubulin intensity) from ten cells per condition. Each plot contains data reflecting the percentage of each type of gradient in that condition (for example, the control RNAi plot is from seven strong, two moderate, and one weak/undetectable). Control RNAi, n = 35 cells; AAK RNAi, n = 45 cells; Tau-nonPhospho, n = 41 cells.

Scale bars, 10 μm (A, E, and I) and 5 μm (B and G). Error bars indicate the SEM. Two-tailed p values of a Student's t test are reported: *$p < 0.05$, **$p < 0.005$, ***$p < 0.0005$. See also Figure S1 and Movie S1.

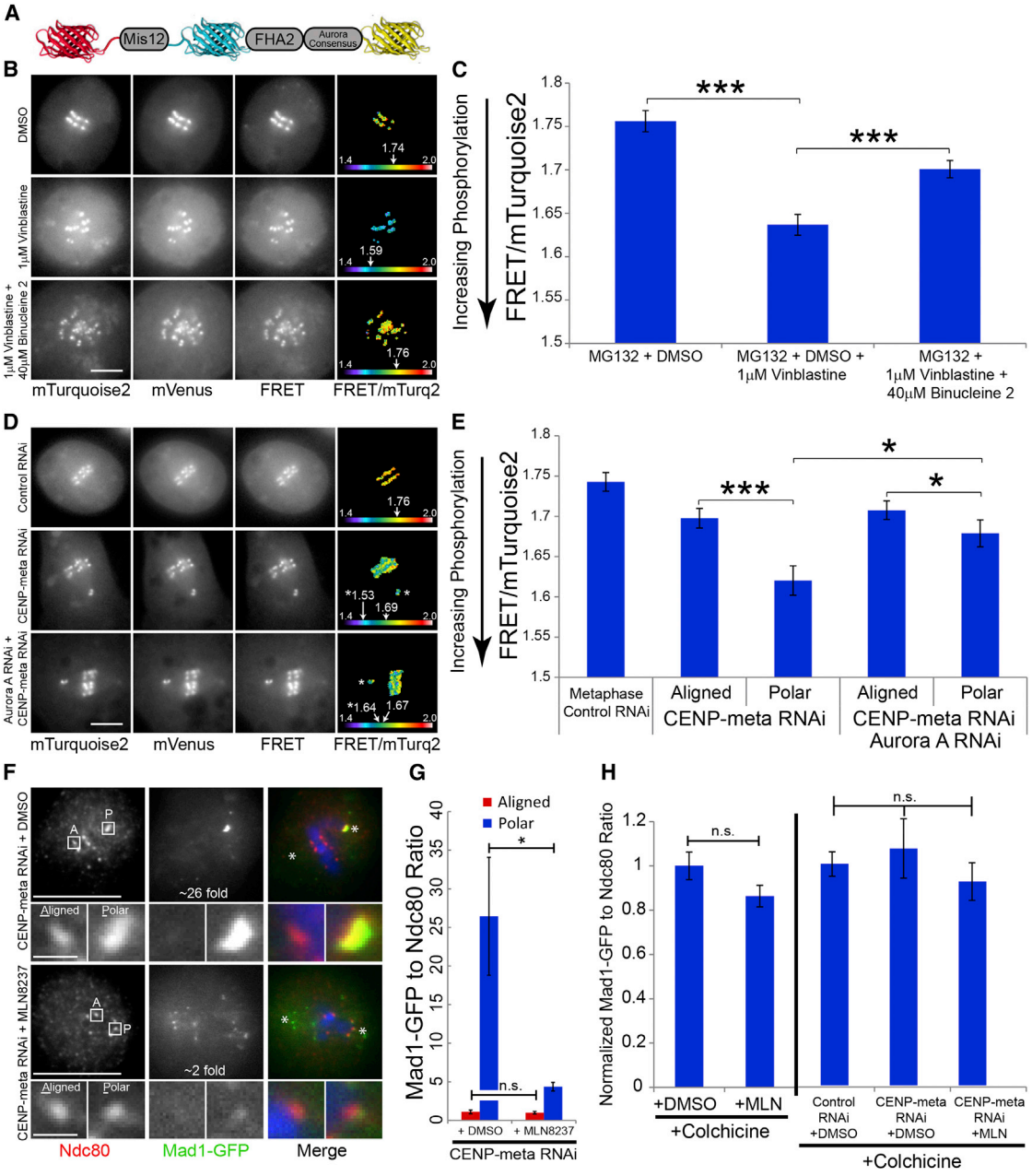

Figure 2. AAK Contributes to Elevated Levels of Kinetochore Phosphorylation and Reduced Kinetochore-MT Attachment Stability near Spindle Poles

(A) Schematic of the kinetochore-targeted Mis12-Aurora FRET sensor used in this study.

(B) Representative images of the FRET reporter in the conditions shown in (C). The FRET emission ratio images "FRET/mTurq2" are pseudo-colored and the arrows point to the position on the color wedge (spanning ratio values of 1.4 to 2.0) corresponding to the average emission ratio measured for the kinetochore-targeted sensor in that cell.

(C) Vinblastine treatment, to generate unattached kinetochores, lowers the emission ratio of the FRET reporter, indicating that it is more phosphorylated. Binucleine 2 treatment leads to an increase in the reporter FRET emission ratio at kinetochores in vinblastine-treated cells, demonstrating that ABK contributes to phosphorylation of the sensor at unattached kinetochores. Mean values from three independent experiments are shown. DMSO, n = 106 cells; vinblastine, n = 104 cells; vinblastine + binucleine 2, n = 108 cells.

(D) Representative images of the FRET reporter in the conditions shown in (E). The FRET emission ratio images "FRET/mTurq2" are pseudo-colored, and the arrows point to the position on the color wedge (spanning ratio values of 1.4 to 2.0) corresponding to the FRET emission ratios measured for the sensor at aligned and, when appropriate, polar kinetochores (asterisk) in that cell.

(E) The mean FRET emission ratio of the sensor is lower at polar kinetochores, generated by depletion of CENP-meta, than at aligned kinetochores. Co-depletion of AAK leads to an increase in the emission ratio at polar kinetochores compared to polar kinetochores in CENP-meta-depleted cells. Thus, the sensor is more phosphorylated at kinetochores near spindle poles than at bioriented kinetochores, and AAK contributes to this difference in the phosphorylation state. Mean

(legend continued on next page)

remained in AAK-depleted cells (Figure 2E). Unfortunately, the effects of binucleine 2 on FRET measurements (Figure S2B) combined with catastrophic failure in bipolar spindle assembly in ABK-inhibited S2 cells made it technically infeasible to measure FRET ratios at polar versus bioriented attachments in ABK-inhibited cells. Nonetheless, the data support the conclusion that an AAK activity gradient contributes to phosphorylation of the Mis12-FRET sensor at polar kinetochores in S2 cells.

The checkpoint protein Mad1, which is depleted from stable kinetochore-MT attachments [33], was next used to probe the attachment states of polar kinetochores in the presence and absence of AAK activity. Mad1 levels at kinetochores were examined in CENP-meta-depleted cells expressing Mad1-GFP under the control of its endogenous promoter (Figures 2F and 2G). To measure Mad1 enrichment at polar kinetochores, we compared the ratio of background corrected fluorescence intensities of Mad1-GFP to Ndc80 signals at misaligned kinetochores to the average Mad1 to Ndc80 ratio intensities of six bioriented kinetochores within the same cell. Indicative of a lack of attachment [32], polar kinetochores, on average, exhibited an ~26-fold increase in Mad1 levels relative to bioriented attachments in CENP-meta-depleted cells treated with DMSO. Treatment with 125 nM MLN8237, an AAK-specific inhibitor [34] that potently and specifically inhibits *Drosophila* AAK (Figures S3A–S3C), caused a significant reduction in Mad1 enrichment (~4-fold) at polar kinetochores. The observed differences in kinetochore-associated Mad1 levels were not due to general effects of the treatments on Mad1 localization as neither MLN-treatment, CENP-meta depletion, or the combination affected Mad1 loading at unattached kinetochores (Figure 2H). These findings along with recent work [35] suggest that polar kinetochores in CENP-meta-depleted cells establish more stable attachments when AAK is inhibited.

Chromosome alignment and kinetochore-MT attachment states were next examined in cells with compromised AAK activity. Similar to previous observations in S2 cells [36], AAK depletion resulted in ~40% of MG132-treated mitotic cells exhibiting "abnormal metaphases" with at least one misaligned chromosome (Figures 3A and 3B). Treatment with 125 nM MLN8237 mirrored the AAK RNAi depletion phenotype (Figures 3C and 3D). The attachment states of misaligned chromosomes were evaluated by careful examination of serial fluorescent z sections of chromosomes, kinetochores, and MTs in control and AAK-inhibited cells (Figures 3E–3H). The attachment states of the misaligned chromosomes fell into four categories: (1) "mono-oriented (k-fiber)" if one kinetochore was attached to a pole and the other kinetochore was nucleating a second kinetochore fiber (k-fiber) or focused spindle pole extending into the cytoplasm, (2) "mono-oriented/lateral" if one kinetochore was attached to a pole and its sister was either unattached or was laterally interacting with a nearby k-fiber (most likely in the process of CENP-E-mediated congression [37]), (3) "syntelic" if sister kinetochores were attached to the same pole, and (4) "unknown" if the attachment state could not be discerned. Once again, the MLN8237 treatment phenocopied AAK RNAi (Figures 3F and 3H). In both conditions, the majority of misaligned chromosomes (50%–60%) had syntelic attachments and 25%–30% had mono-oriented/lateral interactions, suggesting that CENP-meta is active in AAK-inhibited S2 cells. A role for AAK in error correction was further evidenced by the observation that the PEF effect was more potent in AAK-depleted cells relative to control RNAi cells (Figures S3D–S3F). The fixed cell data were corroborated by live-cell imaging of AAK depleted Ndc80-GFP expressing cells (Figure 3I and Movie S3). In an excellent example that captured the chromosome misalignment types observed in fixed AAK-inhibited cells, a syntelically attached chromosome remained "pinned" at the spindle pole for at least 40 min before congressing, most likely via a mono-oriented/lateral interaction, at a rate consistent with CENP-E-driven congression [37]. One of the sister kinetochores then became merotelically attached to both poles, laterally deformed, and briefly lagged in anaphase before properly segregating.

To investigate whether the contribution of AAK to error correction is conserved beyond *Drosophila*, we used PtK1 cells, which, due to their low chromosome number, have been an excellent model for characterizing error correction mechanisms [3, 6]. First, we identified a concentration (1 μM) of the AAK inhibitor MLN8054 [38] that affected chromosome behavior but did not alter mitotic index, distribution of mitotic stages, or spindle assembly (Figures S4A–S4C). PtK1 cells treated with 1 μM MLN8054 did not exhibit a reduction in centromere-associated phosphorylated-ABK (Figure S4D), indicating that ABK activity was not affected by this drug concentration. However, kinetochores in MLN8054-treated prometaphase cells were, on average, positioned closer to the spindle poles than in untreated cells and a significant number of kinetochores localized very close to the poles, which was never observed in control cells (Figures 4A and 4B). Moreover, MLN8054-treated PtK1 cells displayed higher frequencies of merotelic kinetochores at the metaphase plate than control cells (Figures 4C and 4D), and, as a result, significantly more anaphase

values from three independent experiments are shown. Control RNAi, metaphase n = 119 cells; CENP-meta RNAi, aligned n = 98, polar n = 107; CENP-meta, AAK double RNAi, aligned n = 106, polar n = 120.

(F) Single planes from representative images of CENP-meta-depleted Mad1-GFP (green in merged images) expressing cells treated with DMSO or 125 nM MLN8237 and stained for Ndc80 (red) and DAPI (blue). Examples of aligned (A) and polar (P) kinetochores for each condition are shown in the (5× zoom) insets. The fold enrichments of Mad1 at the polar relative to aligned kinetochores are indicated in the Mad1-GFP images for each cell. Asterisks indicate the position of the spindle poles.

(G) Quantifications of fold Mad1-GFP enrichment at polar kinetochores in CENP-meta-depleted cells treated with DMSO (control) or 125 nM MLN8237. Mean values are shown. CENP-meta RNAi + DMSO, n = 18 polar kinetochores, n = 42 aligned kinetochores; CENP-meta RNAi + MLN, n = 46 polar kinetochores, n = 48 aligned kinetochores.

(H) Levels of Mad1-GFP ratioed to Ndc80 at unattached kinetochores are unaffected by MLN treatment and CENP-meta depletion. Mean values from two independent experiments are shown. Colchicine +: DMSO, n = 255 kinetochores; MLN8237, n = 255 kinetochores; control RNAi + DMSO, n = 200 kinetochores; CENP-meta RNAi + DMSO, n = 198 kinetochores; CENP-meta RNAi + MLN8237, n = 200 kinetochores.

All error bars indicate the SEM. Scale bars, 5 μm (B and D), 10 μm (F), and 1 μm (F, insets). Two-tailed p values of a Student's t test are reported in (C), (G), and (H), and p values from a Mann-Whitney Wilcoxon t test are reported in (E): not significant (n.s.) $p > 0.05$, *$p < 0.05$, ***$p < 0.0005$. See also Figure S2.

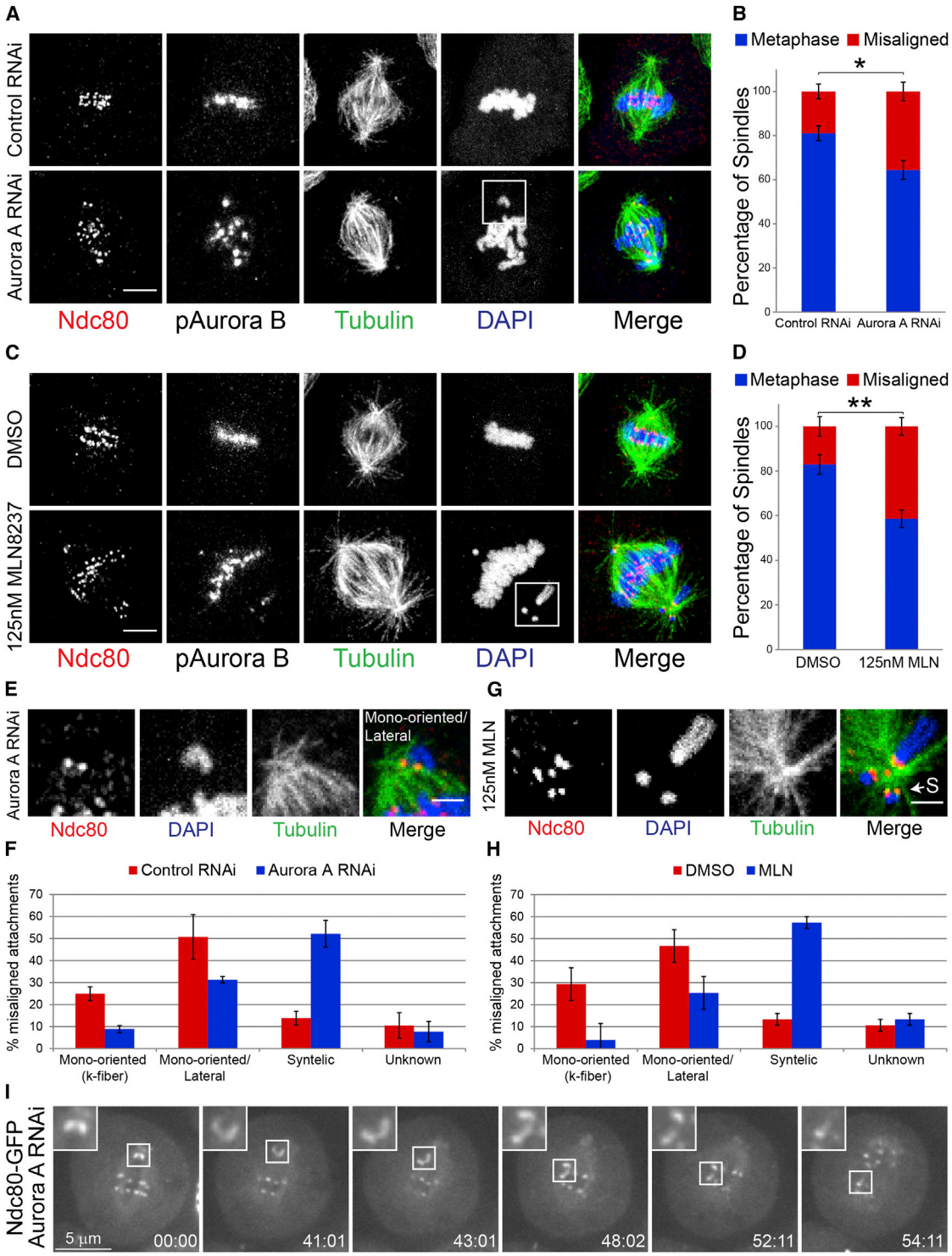

Figure 3. AAK Is Required for Efficient Error Correction in *Drosophila* S2 Cells

(A) Representative maximum-intensity projections from confocal z sections of control and AAK-depleted cells stained for Ndc80 (red in the merged image), phospho-ABK, tubulin (green), and DAPI (blue). Misaligned chromosomes with normal levels of centromere-enriched phospho-ABK are more prevalent in AAK-depleted cells than in control cells.

(B) Quantification of the percentage of MG132-treated cells with normal metaphase plates and misaligned chromosomes in control and AAK-depleted cells. Mean values from three independent experiments are shown. Control RNAi, n = 317 cells; AAK RNAi, n = 326 cells.

(C) Representative maximum-intensity projections from confocal z sections of DMSO- and MLN8237-treated cells stained for Ndc80 (red in the merged image), phospho-ABK, tubulin (green), and DAPI (blue). Treatment with 125 nM MLN8237 phenocopies AAK depletion.

(legend continued on next page)

lagging chromosomes were observed in MLN8054-treated cells (Figure 4E). These data demonstrate that inhibition of AAK compromises error correction and results in chromosome mis-segregation in mammalian PtK1 cells.

We reasoned that AAK regulates error correction by targeting many of the same substrates as ABK. A crucial target of ABK is the Ndc80 complex, which directly binds MTs [10, 11, 39, 40]. High-affinity interactions between the Ndc80 complex and MTs requires the unstructured and highly basic N-terminal tail of Ndc80/Hec1 [11, 40–42], which contains numerous ABK sites [10–12, 22] that, when phosphorylated, lower the complex's affinity for MTs [10, 11, 17]. Thus, we examined the contribution of AAK to the phosphorylation of a previously defined ABK site in Ndc80/Hec1 (Ser55) [10–12] by using a phospho-specific antibody against pSer55 in HeLa cells. Compared to control cells, treatment with 300 nM MLN8237 significantly reduced kinetochore pSer55 staining at attached (Figures 4F and 4G) and unattached kinetochores (Figures S4E and S4F). The 300 nM MLN8237 treatment caused a minor but significant reduction in Ndc80 levels relative to CENP-A (Figures S4G and S4H), which may be due to partial inhibition of ABK at this inhibitor concentration, although phospho-H3-Ser10 levels were not significantly reduced relative to control metaphase cells (Figure S4I). These data are consistent with a phospho-proteomic study that implicated AAK as the primary kinase targeting Ndc80-Ser55 [43]. Although cell-based inhibitor studies suggest that AAK contributes to phosphorylation of Ser55, they are not a direct demonstration of AAK-mediated phosphorylation. To test whether AAK directly phosphorylates Ser55, we performed an in vitro phosphorylation assay with recombinant bonsai Ndc80 complex [11] and purified AAK. When incubated with the bonsai Ndc80 complex in phosphorylation buffer, AAK efficiently phosphorylated Ser55 (Figure 4H). Finally, to examine the spatial contribution of AAK activity to phosphorylation of Ndc80-Ser55, we used the CENP-E inhibitor [44] GSK923295 to generate polar and aligned kinetochores in HeLa cells in the presence and absence of MLN8237 (Figure 4I). In agreement with the S2 cell findings, polar kinetochores were more phosphorylated than aligned/away from the pole kinetochores, and the polar bias in phosphorylation was lost when cells were treated with 300 nM MLN8237 (Figure 4J). Although these findings do not exclude a role for ABK in phosphorylating Ndc80-Ser55 or other kinetochore substrates in the vicinity of spindle poles, taken together, the data demonstrate that AAK can directly phosphorylate Ndc80-Ser55 and that AAK activity contributes to phosphorylation of this residue in HeLa cells.

DISCUSSION

While it has been postulated that AAK could create a kinetochore-MT attachment destabilizing environment near spindle poles [45], it has not been demonstrated experimentally. Here we directly test this hypothesis, and our findings support the existence of a pole-centered AAK phosphorylation gradient that contributes to error correction and counters the potential side effects of elevated PEFs. We envision that superimposed PEF and AAK gradients create a balance of activities near spindle poles that promotes error correction, congression, and biorientation resulting in a spatiotemporal path from mal- to bioriented chromosomes (Figure 4K). First, as an erroneous attachment moves poleward, it may become stabilized by progressively higher levels of opposing PEFs. Second, at some distance from the pole, the PEF effect is countered by an AAK gradient that phosphorylates attachment factors such as the Ndc80 complex. Third, AAK facilitates congression by biasing CENP-E activity, which has been shown to be phospho-regulated near spindle poles by Aurora kinases [46], toward the mid-spindle and by allowing PEFs to push chromosomes away from poles. Note that in this model, production of an unattached kinetochore(s) by AAK is not only a prerequisite for biorientation, but also permits PEFs to congress chromosomes without generating unwanted tension at incorrect attachments.

Both the CEN- and pole-based pathways are spatial positioning phenomena, with the CEN-based system depending on positioning of kinetochore targets relative to ABK and the pole-based pathway relying on spatial positioning of kinetochores relative to spindle poles and AAK. Although both error correction pathways are likely to share common targets (e.g., Ndc80/Hec1), we view the CEN-based pathway as kinetochore intrinsic because the correction machinery (ABK) localizes to the kinetochore region, whereas the pole-based pathway is kinetochore extrinsic since the correction machinery is primarily enriched outside the kinetochore region at the spindle poles/centrosomes. There may be orders of magnitude difference in the working distances of the CEN- and pole-based systems, as changes in spatial separation occur on the nanometer [13–17, 47] and micrometer scale [6], respectively. It will be worthwhile to characterize how the working distance of the pole-based AAK gradient is defined. Although *Drosophila* TPX2 does not regulate AAK [48], in other organisms, TPX2, which localizes AAK to spindle microtubules [49] and activates its kinase activity [50, 51], may help delineate and amplify an AAK gradient [52].

(D) Quantification of the percentage of MG132-treated cells with normal metaphase plates and misaligned chromosomes in DMSO- and MLN8237-treated cells. Mean values from three independent experiments are shown. DMSO, n = 318 cells; 125 nM MLN8237, n = 322 cells.

(E) Zoomed views of the insets highlighted in the DAPI channel in (A). In the merged image, Ndc80 is red, tubulin is green, and DAPI is blue.

(F) Mean values of each type of attachment at misaligned chromosomes in control and AAK-depleted cells from three independent experiments. Control RNAi, n = 71 kinetochore pairs; AAK RNAi, n = 80 kinetochore pairs.

(G) Zoomed views of the insets highlighted in the DAPI channel in (C). In the merged image, Ndc80 is red, tubulin is green, and DAPI is blue. The arrow points to a syntelic (S) attachment.

(H) Mean values of each type of attachment at misaligned chromosomes in DMSO- and MLN8237-treated cells from three independent experiments. n = 75 kinetochore pairs each for the DMSO and MLN conditions.

(I) Still frames from a spinning disk confocal time-lapse of an Ndc80-GFP-expressing S2 cell depleted of AAK. Insets show an 8× zoom of the highlighted regions.

Error bars indicate the SEM. Scale bars, 5 μm (A and C) and 2 μm (E and G). Two-tailed p values of a Student's t test are reported: *$p < 0.05$, **$p < 0.005$. See also Figure S3 and Movie S3.

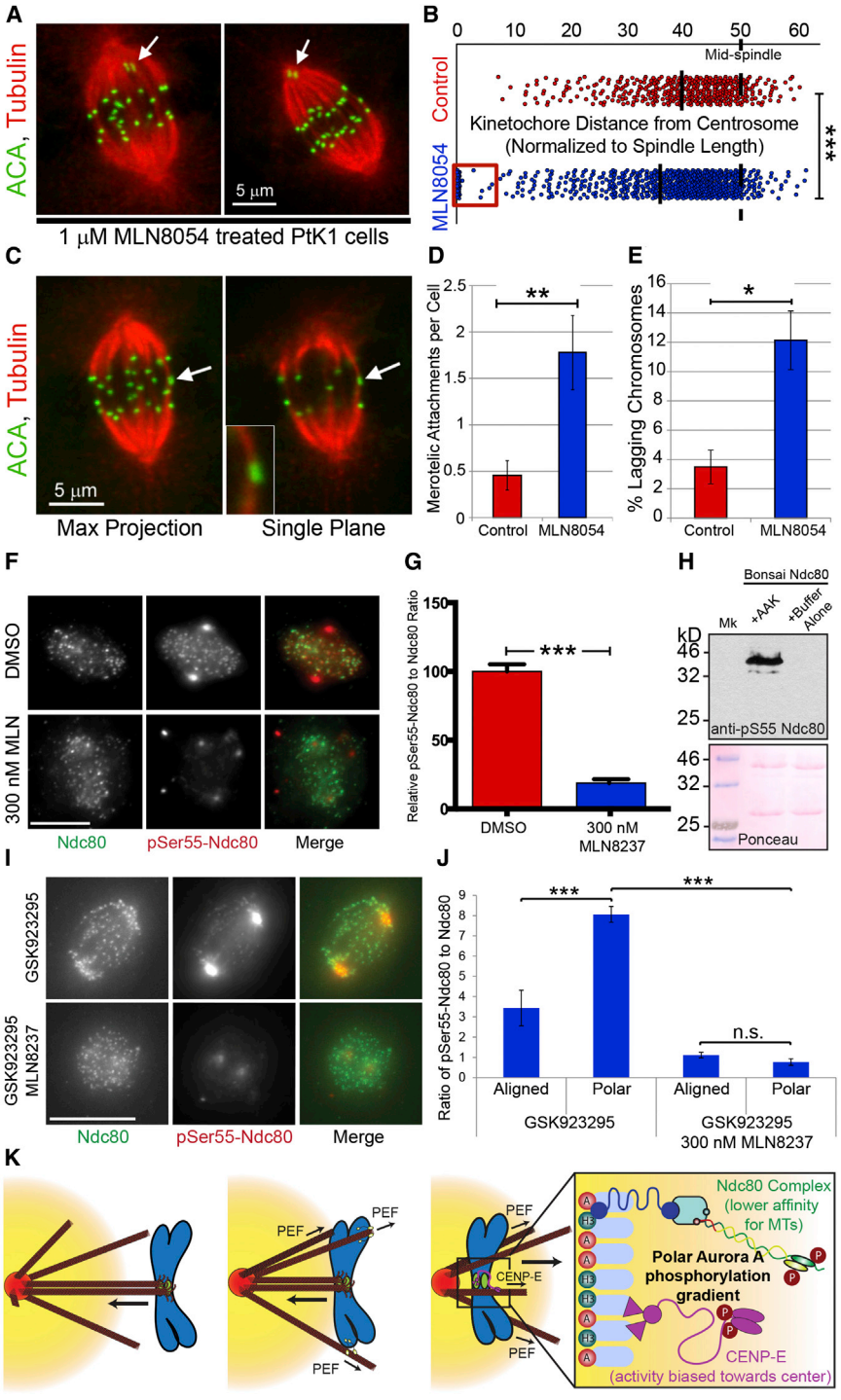

Figure 4. AAK Contributes to Error Correction in Mammalian Cells and Phosphorylates the N-Terminal Tail of Ndc80/Hec1 in Human Cells

(A) Representative maximum-intensity projections of confocal z sections of PtK1 cells treated with 1 μM MLN8054 and stained for tubulin (red) and centromeres (green). Arrows point to polar, mis-aligned chromosomes.

(B) Scatter plots of relative kinetochore positions normalized to the spindle length in control and MLN8054-treated PtK1 cells. The "0" position represents the spindle pole, and the "50" position marks the mid-spindle (dashed black line). The average centromere position (black bar) is closer to the spindle poles in MLN8054-treated cells than in control cells, and a significant population of kinetochores are "pinned" to the poles (near 0) in MLN8054-treated cells (red box). Control, n = 406 kinetochores; 1 μM MLN8054, n = 642 kinetochores.

(C) Representative images (left, maximum-intensity projection; right, single focal plane) of a PtK1 cell treated with 1 μM MLN8054 and stained for tubulin (red) and centromeres (green). Arrows point to a merotelic kinetochore at the metaphase plate that is attached to both spindle poles.

(D) MLN8054 treatment leads to a significant increase in the average number of merotelic attachments per cell relative to control cells. Control, n = 191 kinetochores from 11 cells; 1 μM MLN8054, n = 144 kinetochores from nine cells.

(E) MLN8054 treatment leads to a significant increase in the percentage of lagging chromosomes in anaphase cells relative to control cells. Mean values of lagging chromosomes from three independent experiments are shown. Control, n = 270 anaphase chromosomes; 1 μM MLN8054, n = 268 anaphase chromosomes.

(F) Representative images of control (DMSO) and AAK-inhibited (300 nM MLN8237) HeLa cells stained for pSer55-Ndc80 (red) and Ndc80 (green).

(G) Mean values of pSer55-Ndc80 to Ndc80 ratios. DMSO, n = 280 kinetochores from 14 cells; 300 nM MLN, n = 275 kinetochores from 12 cells.

(H) An in vitro phosphorylation assay with purified Ndc80 bonsai complex plus and minus purified AAK blotted for anti-pSer55. AAK directly phosphorylates Ndc80 in vitro.

(I) Representative images of GSK923295-treated HeLa cells with and without MLN8237 stained for pSer55-Ndc80 (red) and Ndc80 (green).

(J) Polar kinetochores are more phosphorylated than aligned kinetochores in GSK923295-treated cells, and the polar bias in Ser55 phosphorylation is lost in the presence of MLN8237. Mean values are shown. pSer55-Ndc80 to Ndc80 ratios from four independent experiments for GSK923295, aligned n = 408 kinetochores from 68 cells, polar n = 239 kinetochores from 68 cells; three independent experiments for GSK923295 + MLN 8237, aligned n = 465 kinetochores from 55 cells, polar n = 207 kinetochores from 55 cells.

(K) A spatiotemporal model for the path from mal- to bioriented chromosomes. As a syntelic attachment moves poleward, it becomes stabilized as it encounters increasing PEFs, until encountering the AAK phosphorylation gradient. AAK mediates error correction by phosphorylating kinetochore-MT attachment factors such as Ndc80/Hec1 at Ser55. The AAK gradient also facilitates congression by biasing CENP-E activity toward the mid-spindle and by allowing PEFs to push chromosome arms away from the poles without stabilizing syntelic attachments.

Error bars indicate the SEM. Scale bars, 5 μm (A and C) and 10 μm (F and I). Two-tailed p values of a Student's t test are reported: not significant (n.s.) $p > 0.05$, *$p < 0.05$, **$p < 0.005$, ***$p < 0.0005$. See also Figure S4.

Regardless of the effective range of AAK activity, we propose that a key difference between the two pathways is that tension opposes CEN-based error correction, whereas the pole-based pathway is regulated not by tension, but by positioning kinetochores within the spindle relative to the poles. The pole-based error correction pathway appears to be conserved in meiotic cells as a concurrent study using mouse oocytes found that AAK activity contributes to destabilizing kinetochore-MT attachments near spindle poles [53].

It is imperative that mal-oriented chromosomes near spindle poles are corrected, because whereas only a fraction of merotelic kinetochores at the metaphase plate result in chromosome mis-segregation [54], mitotic progression in the presence of polar chromosomes would inevitably lead to aneuploidy. Furthermore, we view the consequences of inhibiting AAK-mediated error correction not merely as more subtle than the effects of ABK inhibition, but as more insidious. Although catastrophic failure in error correction, like that seen after potent ABK inhibition, would lead to massive and most likely lethal aneuploidy, the presence of comparatively low numbers of ''pinned'' polar chromosomes when the AAK pathway is compromised would increase the frequency of single chromosome mis-segregation events and be more likely to yield viable aneuploid cells. Our findings support the conclusion that an AAK phosphorylation gradient contributes to correcting such hazardous polar attachments before cells divide.

EXPERIMENTAL PROCEDURES

Experimental procedures are described in the Supplemental Information.

SUPPLEMENTAL INFORMATION

Supplemental Information includes Supplemental Experimental Procedures, four figures, one table, and three movies and can be found with this article online at http://dx.doi.org/10.1016/j.cub.2015.06.021.

AUTHOR CONTRIBUTIONS

T.J.M. conceived of the project, carried out experiments and analyses, and wrote the paper. A.A.Y. conducted and analyzed most of the *Drosophila* cell experiments. C.M.H. performed experiments examining Mad1 localization and characterizing the specificity of MLN8237 in *Drosophila* cells. D.C. and A.W.H. designed and performed experiments and analyses with PtK1 cells. J.P.W. and J.D. performed all HeLa cell experiments and analyses. Text was contributed by D.C., J.P.W., C.M.H., and A.A.Y. The manuscript was edited by T.J.M., D.C., J.P.W., A.A.Y., and C.M.H.

ACKNOWLEDGMENTS

We thank Marcin Przewloka and David Glover for the generous gift of the *Drosophila* anti-Aurora A, Iain Cheeseman for anti-bonsai-Ndc80, and Jennifer DeLuca for the phospho-ABK antibody. We are grateful to Michael Lampson, Jennifer DeLuca, and Iain Cheeseman for communicating unpublished findings. We also acknowledge Ted Salmon and members of the J.P.W., D.C., Lee, Wadsworth, and T.J.M. labs for thoughtful scientific discussions. We thank Julia Torabi for generating the Tau-FRET sensors. This work was supported by an NIH grant (5 R01 GM107026) to T.J.M and by Research Grant No. 5-FY13-205 from the March of Dimes Foundation to T.J.M, as well as by the Charles H. Hood Foundation (T.J.M.). The work was also partly funded by NSF grant MCB-0842551 to D.C. A.W.H was the recipient of a VT-IMSD Undergraduate Research Apprenticeship. J.P.W. is supported by a CRUK Career Development Fellowship (C40377/A12840). J.D. is supported by a Darwin Trust Studentship.

Received: April 1, 2015
Revised: June 8, 2015
Accepted: June 9, 2015
Published: July 9, 2015

REFERENCES

1. Cimini, D., Moree, B., Canman, J.C., and Salmon, E.D. (2003). Merotelic kinetochore orientation occurs frequently during early mitosis in mammalian tissue cells and error correction is achieved by two different mechanisms. J. Cell Sci. *116*, 4213–4225.
2. Kitajima, T.S., Ohsugi, M., and Ellenberg, J. (2011). Complete kinetochore tracking reveals error-prone homologous chromosome biorientation in mammalian oocytes. Cell *146*, 568–581.
3. Cimini, D., Wan, X., Hirel, C.B., and Salmon, E.D. (2006). Aurora kinase promotes turnover of kinetochore microtubules to reduce chromosome segregation errors. Curr. Biol. *16*, 1711–1718.
4. Kelly, A.E., and Funabiki, H. (2009). Correcting aberrant kinetochore microtubule attachments: an Aurora B-centric view. Curr. Opin. Cell Biol. *21*, 51–58.
5. Tanaka, T.U., Rachidi, N., Janke, C., Pereira, G., Galova, M., Schiebel, E., Stark, M.J., and Nasmyth, K. (2002). Evidence that the Ipl1-Sli15 (Aurora kinase-INCENP) complex promotes chromosome bi-orientation by altering kinetochore-spindle pole connections. Cell *108*, 317–329.
6. Lampson, M.A., Renduchitala, K., Khodjakov, A., and Kapoor, T.M. (2004). Correcting improper chromosome-spindle attachments during cell division. Nat. Cell Biol. *6*, 232–237.
7. Ke, K., Cheng, J., and Hunt, A.J. (2009). The distribution of polar ejection forces determines the amplitude of chromosome directional instability. Curr. Biol. *19*, 807–815.
8. Cane, S., Ye, A.A., Luks-Morgan, S.J., and Maresca, T.J. (2013). Elevated polar ejection forces stabilize kinetochore-microtubule attachments. J. Cell Biol. *200*, 203–218.
9. Nicklas, R.B., and Koch, C.A. (1969). Chromosome micromanipulation. 3. Spindle fiber tension and the reorientation of mal-oriented chromosomes. J. Cell Biol. *43*, 40–50.
10. Cheeseman, I.M., Chappie, J.S., Wilson-Kubalek, E.M., and Desai, A. (2006). The conserved KMN network constitutes the core microtubule-binding site of the kinetochore. Cell *127*, 983–997.
11. Ciferri, C., Pasqualato, S., Screpanti, E., Varetti, G., Santaguida, S., Dos Reis, G., Maiolica, A., Polka, J., De Luca, J.G., De Wulf, P., et al. (2008). Implications for kinetochore-microtubule attachment from the structure of an engineered Ndc80 complex. Cell *133*, 427–439.
12. DeLuca, J.G., Gall, W.E., Ciferri, C., Cimini, D., Musacchio, A., and Salmon, E.D. (2006). Kinetochore microtubule dynamics and attachment stability are regulated by Hec1. Cell *127*, 969–982.
13. Maresca, T.J., and Salmon, E.D. (2009). Intrakinetochore stretch is associated with changes in kinetochore phosphorylation and spindle assembly checkpoint activity. J. Cell Biol. *184*, 373–381.
14. Uchida, K.S., Takagaki, K., Kumada, K., Hirayama, Y., Noda, T., and Hirota, T. (2009). Kinetochore stretching inactivates the spindle assembly checkpoint. J. Cell Biol. *184*, 383–390.
15. Liu, D., Vader, G., Vromans, M.J., Lampson, M.A., and Lens, S.M. (2009). Sensing chromosome bi-orientation by spatial separation of aurora B kinase from kinetochore substrates. Science *323*, 1350–1353.
16. Suzuki, A., Badger, B.L., Wan, X., DeLuca, J.G., and Salmon, E.D. (2014). The architecture of CCAN proteins creates a structural integrity to resist spindle forces and achieve proper Intrakinetochore stretch. Dev. Cell *30*, 717–730.
17. Welburn, J.P., Vleugel, M., Liu, D., Yates, J.R., 3rd, Lampson, M.A., Fukagawa, T., and Cheeseman, I.M. (2010). Aurora B phosphorylates spatially distinct targets to differentially regulate the kinetochore-microtubule interface. Mol. Cell *38*, 383–392.

18. Maresca, T.J., and Salmon, E.D. (2010). Welcome to a new kind of tension: translating kinetochore mechanics into a wait-anaphase signal. J. Cell Sci. *123*, 825–835.
19. Cassimeris, L., Rieder, C.L., and Salmon, E.D. (1994). Microtubule assembly and kinetochore directional instability in vertebrate monopolar spindles: implications for the mechanism of chromosome congression. J. Cell Sci. *107*, 285–297.
20. Campbell, C.S., and Desai, A. (2013). Tension sensing by Aurora B kinase is independent of survivin-based centromere localization. Nature *497*, 118–121.
21. Carmena, M., and Earnshaw, W.C. (2003). The cellular geography of aurora kinases. Nat. Rev. Mol. Cell Biol. *4*, 842–854.
22. Cheeseman, I.M., Anderson, S., Jwa, M., Green, E.M., Kang, Js., Yates, J.R., 3rd, Chan, C.S., Drubin, D.G., and Barnes, G. (2002). Phospho-regulation of kinetochore-microtubule attachments by the Aurora kinase Ipl1p. Cell *111*, 163–172.
23. Li, S., Deng, Z., Fu, J., Xu, C., Xin, G., Wu, Z., Luo, J., Wang, G., Zhang, S., Zhang, B., et al. (2015). Spatial compartmentalization specializes function of Aurora-A and Aurora-B. J. Biol. Chem. Published online May 18, 2015. http://dx.doi.org/10.1074/jbc.M115.652453.
24. Theurkauf, W.E., and Hawley, R.S. (1992). Meiotic spindle assembly in Drosophila females: behavior of nonexchange chromosomes and the effects of mutations in the nod kinesin-like protein. J. Cell Biol. *116*, 1167–1180.
25. Stenoien, D.L., Sen, S., Mancini, M.A., and Brinkley, B.R. (2003). Dynamic association of a tumor amplified kinase, Aurora-A, with the centrosome and mitotic spindle. Cell Motil. Cytoskeleton *55*, 134–146.
26. Violin, J.D., Zhang, J., Tsien, R.Y., and Newton, A.C. (2003). A genetically encoded fluorescent reporter reveals oscillatory phosphorylation by protein kinase C. J. Cell Biol. *161*, 899–909.
27. Fuller, B.G., Lampson, M.A., Foley, E.A., Rosasco-Nitcher, S., Le, K.V., Tobelmann, P., Brautigan, D.L., Stukenberg, P.T., and Kapoor, T.M. (2008). Midzone activation of aurora B in anaphase produces an intracellular phosphorylation gradient. Nature *453*, 1132–1136.
28. Tseng, B.S., Tan, L., Kapoor, T.M., and Funabiki, H. (2010). Dual detection of chromosomes and microtubules by the chromosomal passenger complex drives spindle assembly. Dev. Cell *18*, 903–912.
29. Eggert, U.S., Kiger, A.A., Richter, C., Perlman, Z.E., Perrimon, N., Mitchison, T.J., and Field, C.M. (2004). Parallel chemical genetic and genome-wide RNAi screens identify cytokinesis inhibitors and targets. PLoS Biol. *2*, e379.
30. Smurnyy, Y., Toms, A.V., Hickson, G.R., Eck, M.J., and Eggert, U.S. (2010). Binucleine 2, an isoform-specific inhibitor of Drosophila Aurora B kinase, provides insights into the mechanism of cytokinesis. ACS Chem. Biol. *5*, 1015–1020.
31. Yucel, J.K., Marszalek, J.D., McIntosh, J.R., Goldstein, L.S., Cleveland, D.W., and Philp, A.V. (2000). CENP-meta, an essential kinetochore kinesin required for the maintenance of metaphase chromosome alignment in Drosophila. J. Cell Biol. *150*, 1–11.
32. Putkey, F.R., Cramer, T., Morphew, M.K., Silk, A.D., Johnson, R.S., McIntosh, J.R., and Cleveland, D.W. (2002). Unstable kinetochore-microtubule capture and chromosomal instability following deletion of CENP-E. Dev. Cell *3*, 351–365.
33. Shah, J.V., Botvinick, E., Bonday, Z., Furnari, F., Berns, M., and Cleveland, D.W. (2004). Dynamics of centromere and kinetochore proteins; implications for checkpoint signaling and silencing. Curr. Biol. *14*, 942–952.
34. Pollard, J.R., and Mortimore, M. (2009). Discovery and development of aurora kinase inhibitors as anticancer agents. J. Med. Chem. *52*, 2629–2651.
35. Barisic, M., Aguiar, P., Geley, S., and Maiato, H. (2014). Kinetochore motors drive congression of peripheral polar chromosomes by overcoming random arm-ejection forces. Nat. Cell Biol. *16*, 1249–1256.
36. Giet, R., McLean, D., Descamps, S., Lee, M.J., Raff, J.W., Prigent, C., and Glover, D.M. (2002). Drosophila Aurora A kinase is required to localize D-TACC to centrosomes and to regulate astral microtubules. J. Cell Biol. *156*, 437–451.
37. Kapoor, T.M., Lampson, M.A., Hergert, P., Cameron, L., Cimini, D., Salmon, E.D., McEwen, B.F., and Khodjakov, A. (2006). Chromosomes can congress to the metaphase plate before biorientation. Science *311*, 388–391.
38. Manfredi, M.G., Ecsedy, J.A., Meetze, K.A., Balani, S.K., Burenkova, O., Chen, W., Galvin, K.M., Hoar, K.M., Huck, J.J., LeRoy, P.J., et al. (2007). Antitumor activity of MLN8054, an orally active small-molecule inhibitor of Aurora A kinase. Proc. Natl. Acad. Sci. USA *104*, 4106–4111.
39. Alushin, G.M., Ramey, V.H., Pasqualato, S., Ball, D.A., Grigorieff, N., Musacchio, A., and Nogales, E. (2010). The Ndc80 kinetochore complex forms oligomeric arrays along microtubules. Nature *467*, 805–810.
40. Wei, R.R., Al-Bassam, J., and Harrison, S.C. (2007). The Ndc80/HEC1 complex is a contact point for kinetochore-microtubule attachment. Nat. Struct. Mol. Biol. *14*, 54–59.
41. Guimaraes, G.J., Dong, Y., McEwen, B.F., and Deluca, J.G. (2008). Kinetochore-microtubule attachment relies on the disordered N-terminal tail domain of Hec1. Curr. Biol. *18*, 1778–1784.
42. Miller, S.A., Johnson, M.L., and Stukenberg, P.T. (2008). Kinetochore attachments require an interaction between unstructured tails on microtubules and Ndc80(Hec1). Curr. Biol. *18*, 1785–1791.
43. Kettenbach, A.N., Schweppe, D.K., Faherty, B.K., Pechenick, D., Pletnev, A.A., and Gerber, S.A. (2011). Quantitative phosphoproteomics identifies substrates and functional modules of Aurora and Polo-like kinase activities in mitotic cells. Sci. Signal. *4*, rs5.
44. Wood, K.W., Lad, L., Luo, L., Qian, X., Knight, S.D., Nevins, N., Brejc, K., Sutton, D., Gilmartin, A.G., Chua, P.R., et al. (2010). Antitumor activity of an allosteric inhibitor of centromere-associated protein-E. Proc. Natl. Acad. Sci. USA *107*, 5839–5844.
45. Godek, K.M., Kabeche, L., and Compton, D.A. (2015). Regulation of kinetochore-microtubule attachments through homeostatic control during mitosis. Nat. Rev. Mol. Cell Biol. *16*, 57–64.
46. Kim, Y., Holland, A.J., Lan, W., and Cleveland, D.W. (2010). Aurora kinases and protein phosphatase 1 mediate chromosome congression through regulation of CENP-E. Cell *142*, 444–455.
47. Wan, X., O'Quinn, R.P., Pierce, H.L., Joglekar, A.P., Gall, W.E., DeLuca, J.G., Carroll, C.W., Liu, S.T., Yen, T.J., McEwen, B.F., et al. (2009). Protein architecture of the human kinetochore microtubule attachment site. Cell *137*, 672–684.
48. Goshima, G. (2011). Identification of a TPX2-like microtubule-associated protein in Drosophila. PLoS ONE *6*, e28120.
49. Kufer, T.A., Silljé, H.H., Körner, R., Gruss, O.J., Meraldi, P., and Nigg, E.A. (2002). Human TPX2 is required for targeting Aurora-A kinase to the spindle. J. Cell Biol. *158*, 617–623.
50. Eyers, P.A., Erikson, E., Chen, L.G., and Maller, J.L. (2003). A novel mechanism for activation of the protein kinase Aurora A. Curr. Biol. *13*, 691–697.
51. Tsai, M.Y., Wiese, C., Cao, K., Martin, O., Donovan, P., Ruderman, J., Prigent, C., and Zheng, Y. (2003). A Ran signalling pathway mediated by the mitotic kinase Aurora A in spindle assembly. Nat. Cell Biol. *5*, 242–248.
52. Greenan, G., Brangwynne, C.P., Jaensch, S., Gharakhani, J., Jülicher, F., and Hyman, A.A. (2010). Centrosome size sets mitotic spindle length in Caenorhabditis elegans embryos. Curr. Biol. *20*, 353–358.
53. Chmátal, L., Yang, K., Schultz, R.M., and Lampson, M.A. (2015). Spatial regulation of kinetochore microtubule attachments by destabilization at spindle poles in meiosis I. Curr. Biol. *25*, this issue, 1835–1841.
54. Thompson, S.L., and Compton, D.A. (2011). Chromosome missegregation in human cells arises through specific types of kinetochore-microtubule attachment errors. Proc. Natl. Acad. Sci. USA *108*, 17974–17978.